

X-ray absorption of the negative charge-transfer material $\text{SrFe}_{1-x}\text{Co}_x\text{O}_3$ M. Abbate,¹ G. Zampieri,² J. Okamoto,³ A. Fujimori,⁴ S. Kawasaki,⁵ and M. Takano⁵¹*Departamento de Física, Universidade Federal de Paraná, Caixa Postal 19091, 81531-990 Curitiba PR, Brazil*²*Centro Atómico Bariloche, Comisión Nacional de Energía Atómica, 8400 Bariloche, Rio Negro, Argentina*³*Synchrotron Radiation Research Center, Japan Atomic Energy Research Institute, Hyogo 679-5148, Japan*⁴*Department of Physics, University of Tokyo, Bunkyo-ku, Tokyo 113-0033, Japan*⁵*Institute for Chemical Research, Kyoto University, Uji, Kyoto 611-0011, Japan*

(Received 12 November 2001; revised manuscript received 1 February 2002; published 15 April 2002)

We studied the relation between the electronic structure and the physical properties of $\text{SrFe}_{1-x}\text{Co}_x\text{O}_3$. The main technique used in the study was Fe $2p$, Co $2p$, and O $1s$ x-ray absorption spectroscopy. The experimental spectra were analyzed in terms of the configuration-interaction cluster model calculation. The analysis of the spectra shows that both SrFeO_3 and SrCoO_3 are in the negative-charge transfer regime (this means that their ground states are mostly covalent and contain considerable O $2p$ hole character). SrFeO_3 is in a high-spin state and SrCoO_3 in an intermediate-spin state stabilized by strong hybridization. The local electronic structure and the corresponding spin state are mostly preserved in $\text{SrFe}_{1-x}\text{Co}_x\text{O}_3$. The relatively large O $2p$ hole weight in the ground state explains the absence of Jahn-Teller distortions, as well as the relatively large value of the magnetic moment observed at the O sites in these materials. $\text{SrFe}_{1-x}\text{Co}_x\text{O}_3$ illustrates both ferromagnetism and magneto-resistance in a negative charge-transfer material.

DOI: 10.1103/PhysRevB.65.165120

PACS number(s): 78.70.Dm, 71.30.+h

I. INTRODUCTION

Colossal magnetoresistance (CMR) materials, such as manganites¹ and double perovskites,² are attracting considerable attention. The interest in these materials was originally sparked by their potential applications as magnetic sensors in reading heads. Additional interest was provided by the challenges in the elucidation of the microscopic origin of the CMR mechanism. It is generally invoked that the physical properties of manganites, such as $\text{La}_{1-x}\text{Ca}_x\text{MnO}_3$, are dominated by the double-exchange mechanism.¹ Whereas tunneling magnetoresistance between (half-metallic) ferromagnetic phases was proposed in double-perovskites materials, such as $\text{Sr}_2\text{FeMoO}_6$.²

The $\text{SrFe}_{1-x}\text{Co}_x\text{O}_3$ compound³⁻⁵ also presents a large negative magnetoresistance for a wide concentration range ($0 \leq x \leq 0.7$).⁶ Despite several studies of the physical properties of this system, still very little is known about the electronic structure and the magnetoresistance. The electronic structure of this material is particularly interesting because the transition metal ions are in a relatively high oxidation state. In fact, it is expected that the ground state could be qualitatively different with respect to manganites¹ and double perovskites.² This provided the motivation to investigate the electronic structure of the $\text{SrFe}_{1-x}\text{Co}_x\text{O}_3$ series using direct spectroscopic techniques.

The purpose of this work is to study the relation between the electronic structure and the physical properties of $\text{SrFe}_{1-x}\text{Co}_x\text{O}_3$. The main experimental techniques used in this study were Fe $2p$, Co $2p$, and O $1s$ soft x-ray absorption spectroscopy (XAS). The experimental results were analyzed in terms of combined atomic multiplet, crystal field and cluster model calculations. The analysis of the spectra shows that the electronic structure of these materials is dominated by a negative-charge-transfer character. This means that the ionic state of the Fe and Co ions is not really +4,

but rather that the charge state is compensated by O $2p$ holes.

The structure of the SrFeO_3 perovskite is cubic (space group $Pm\bar{3}m$) with a lattice parameter of $a = 3.845 \text{ \AA}$.³ SrFeO_3 is antiferromagnetic with a screw structure along the $\langle 111 \rangle$ propagation vector. The ordering temperature of stoichiometric SrFeO_3 is $T_N = 134 \text{ K}$ and the Fe magnetic moment is $3.1 \mu_B$.³ SrFeO_3 is metallic ($\partial\rho/\partial T > 0$) down to 4 K and has a room-temperature resistivity of $10^{-3} \Omega \text{ cm}$.³ SrCoO_3 has the cubic perovskite structure (space group $Pm\bar{3}m$) with a lattice parameter of $a = 3.835 \text{ \AA}$.⁴ Stoichiometric SrCoO_3 is ferromagnetic with a Curie temperature of $T_C = 280 \text{ K}$ and the Co magnetic moment is $2.1 \mu_B$.⁴ SrCoO_3 is also metallic ($\partial\rho/\partial T > 0$) down to 4 K and has a room temperature resistivity of about $10^{-3} \Omega \text{ cm}$.⁴

$\text{SrFe}_{1-x}\text{Co}_x\text{O}_3$ remains cubic over the whole composition range with a lattice parameter of $a = 3.835 - 3.845 \text{ \AA}$.⁵ The $\text{SrFe}_{1-x}\text{Co}_x\text{O}_3$ material is metallic ($\partial\rho/\partial T > 0$) with a room-temperature resistivity in the range $10^{-3} - 10^{-4} \Omega \text{ cm}$.⁵ The $\text{SrFe}_{1-x}\text{Co}_x\text{O}_3$ compound is antiferromagnetic for $x \leq 0.10 - 0.15$ and becomes ferromagnetic for $x \geq 0.2$. The Curie temperature T_C increases with x and is maximum around $0.4 \leq x \leq 0.6$, whereas the saturated magnetic moment μ peaks around $0.2 \leq x \leq 0.4$.⁵ In particular, the $\text{SrFe}_{0.5}\text{Co}_{0.5}\text{O}_3$ compound has a $T_C = 340 \text{ K}$ and a saturated magnetic moment of about $3 \mu_B$. Finally, the $\text{SrFe}_{1-x}\text{Co}_x\text{O}_3$ system presents a relatively large negative magnetoresistance for $0 \leq x \leq 0.7$.⁶

II. EXPERIMENTAL DETAILS

The samples studied here were nearly stoichiometric SrFeO_3 , $\text{SrFe}_{0.5}\text{Co}_{0.5}\text{O}_3$, and SrCoO_3 . First, oxygen deficient samples were prepared using the solid-state reaction method. Then, the samples were sealed in gold capsules with the oxygen dispenser KClO_4 . Finally, the samples were

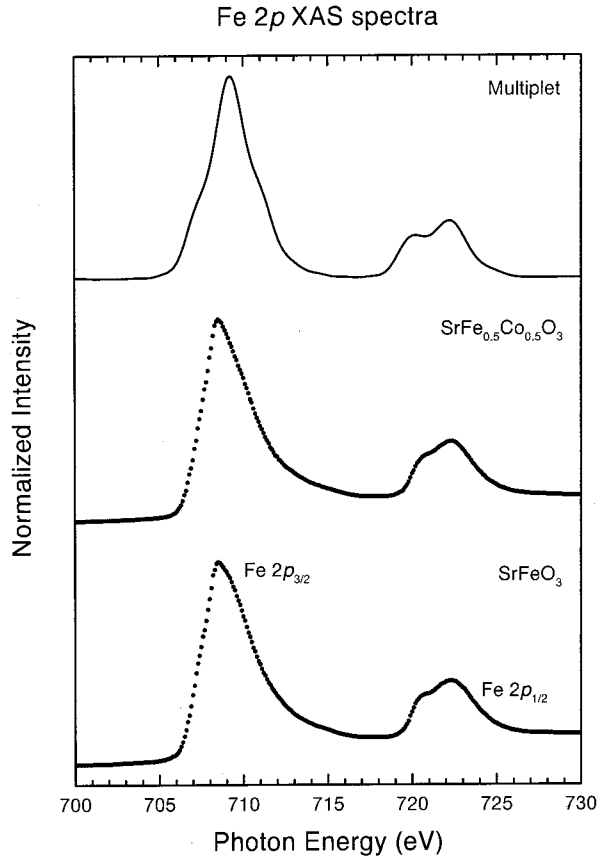


FIG. 1. Fe 2*p* x-ray absorption spectra of SrFeO₃ and SrFe_{0.5}Co_{0.5}O₃ (dots) compared to an atomic multiplet calculation (solid line).

treated at 6 GPa and 600 °C for 30 min. X-ray diffraction analysis showed that all the samples were single phase.⁷ Iodometric titration showed that the oxygen deficiency was less than 1%.⁷ The characterization also included Mössbauer and magnetization measurements.⁷

The XAS measurements were performed at the spherical-grating-monochromator (SGM) beamline in the LNLS. The base pressure in the experimental chamber was in the low 10⁻⁹ mbar range. The samples were scraped *in situ* with a diamond file to remove surface contamination. The spectra were measured using the total-electron-yield (TEY) method. The mean probing depth of soft x-ray absorption using the TEY method is approximately 5 nm.⁸ The energy resolution at the O 1*s* x-ray absorption edge was better than 0.5 eV. The energy scale of the spectra was calibrated using the known peak positions in TiO₂. The spectra were normalized to the maximum after a constant background subtraction.

III. RESULTS AND DISCUSSION

A. Fe 2*p* XAS spectra

Figure 1 shows the Fe 2*p* x-ray absorption (XAS) spectra of SrFeO₃ and SrFe_{0.5}Co_{0.5}O₃. The spectra corresponds to Fe 2*p* → Fe 3*d* transitions and are dominated by multiplet

effects. The spectra are split by the Fe 2*p* spin-orbit interaction into the Fe 2*p*_{3/2} and Fe 2*p*_{1/2} regions. In turn, these regions are further split by Fe 2*p*-3*d* electrostatic interactions and crystal field effects. The shape of the multiples in the spectra are directly related to the ground state of the Fe ions. These spectra can be analyzed in terms of combined atomic multiplet plus crystal field calculations.⁹

The Fe 2*p* XAS spectrum of SrFeO₃ corresponds formally to Fe⁴⁺ (3*d*⁴) ions in a high-spin state. The calculation based on the single ionic configuration *t*_{2*g*}³*e*_g¹ (⁵*E*) does not account for the spectrum.¹⁰ The problem is that the ground state contains not only 3*d*⁴ but also considerable 3*d*⁵ \underline{L} character (where \underline{L} denotes a ligand hole). Therefore, the calculation must include the contributions of the charge-transfer configurations 3*d*⁵ \underline{L} [the main 3*d*⁵ component of the 3*d*⁵ \underline{L} configuration is given by the high-spin *t*_{2*g*}³*e*_g² (⁶*A*₁) state].

The charge-transfer configurations were included using the configuration interaction (CI) method. The ground state of SrFeO₃ was expanded in terms of the 3*d*⁴, 3*d*⁵ \underline{L} , and 3*d*⁶ \underline{L}^2 configurations. The main parameters were the charge-transfer energy Δ , the Mott-Hubbard repulsion *U*, and the transfer integral *T* _{σ} . The value of the parameters were obtained from Ref. 11 ($\Delta=0$ eV, *U*=7.5 eV, and *T* _{σ} =2.2 eV). The occupations of the configurations in the ground state are 36% 3*d*⁴, 58% 3*d*⁵ \underline{L} , and 6% 3*d*⁶ \underline{L}^2 . Figure 1 shows that the CI calculation reproduces reasonably well the features in the SrFeO₃ spectrum [the agreement is better than that obtained using a single ionic configuration *t*_{2*g*}³*e*_g¹ (⁵*E*) calculation, see Ref. 10].

The occupation of the 3*d*⁵ \underline{L} configuration in SrFeO₃ is larger than that of the 3*d*⁴ configuration. This means that SrFeO₃ is in the negative charge-transfer regime with holes in the O 2*p* levels¹² (the effective charge-transfer parameter Δ_{eff} of SrFeO₃ is actually negative due to multiplet splitting). This regime is characteristic of compounds with transition metal ions in relatively high oxidation states. The calculated 3*d* count for SrFeO₃, approximately 4.7, is larger than the purely ionic value 4.0. This indicates that the covalent contribution to the bonding in the SrFeO₃ compound is relatively large.

The Fe 2*p* XAS spectrum of SrFe_{0.5}Co_{0.5}O₃ presents only minor changes with respect to SrFeO₃. The absence of changes indicates that the Fe ions remains relatively unaffected in SrFe_{0.5}Co_{0.5}O₃. This means that the formally tetravalent Fe⁴⁺ ions in the mixed compound are in a high-spin state, that the material is in the negative-charge-transfer regime with a considerable amount of O 2*p* holes, and finally that the covalent contribution to the bonding in SrFe_{0.5}Co_{0.5}O₃ is relatively large. Further support for these conclusions is provided by the analysis of the O 1*s* XAS spectra below.

B. Co 2*p* XAS spectra

Figure 2 shows the Co 2*p* x-ray absorption spectra of SrCoO₃ and SrFe_{0.5}Co_{0.5}O₃. The analysis of the Co 2*p* XAS spectra follow closely that of the Fe 2*p* XAS spectra above. The spectrum of SrCoO₃ corresponds formally to Co⁴⁺

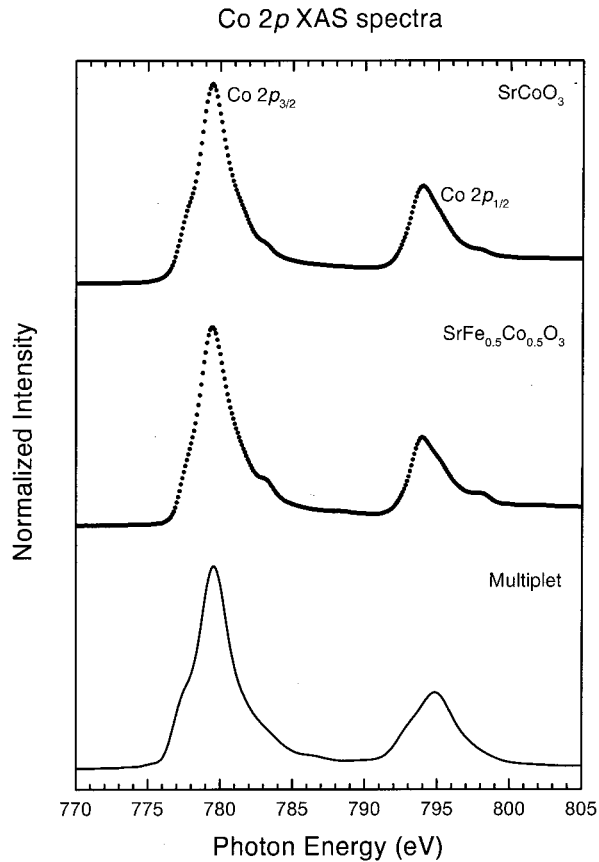


FIG. 2. Co $2p$ x-ray absorption spectra of $\text{SrFe}_{0.5}\text{Co}_{0.5}\text{O}_3$ and SrCoO_3 (dots) compared to an atomic multiplet calculation (solid line).

($3d^5$) ions in an intermediate-spin state. In a purely ionic picture, the ground state of the Co^{4+} should be either high spin or low spin. The $t_{2g}^4 e_g^1$ (4T_1) intermediate-spin state is stabilized by the hybridization with the $3d^6\bar{L}$ configuration¹³ [the main $3d^6$ component of the $3d^6\bar{L}$ configuration is given by the high-spin $t_{2g}^4 e_g^2$ (5T_2) state].

The calculation based on the single ionic configuration does not account for the spectrum of SrCoO_3 . Again, the calculation must include the contributions of the charge-transfer configurations $3d^6\bar{L}$. The ground state of SrCoO_3 was expanded in terms of the $3d^5$, $3d^6\bar{L}$, and $3d^7\bar{L}^2$ configurations. The value of the parameters were obtained from Ref. 13 ($\Delta = -2$ eV, $U = 7.5$ eV, and $T_\sigma = 2.0$ eV). The occupations of the configurations in the ground state are 22% $3d^5$, 67% $3d^6\bar{L}$, and 11% $3d^7\bar{L}^2$. Figure 2 shows that the CI calculation reproduces reasonably well the features in the SrCoO_3 spectrum (the agreement is better than that obtained using either high-spin or low-spin states calculations, see Ref. 13).

The occupation of the $3d^6\bar{L}$ configuration in SrCoO_3 is much larger than that of the $3d^5$ configuration. This means that SrCoO_3 also is in the negative charge-transfer regime with holes in the O $2p$ levels¹² (which is in agreement with the already negative value of the charge-transfer parameter Δ for this compound). The calculated $3d$ count for SrCoO_3 ,

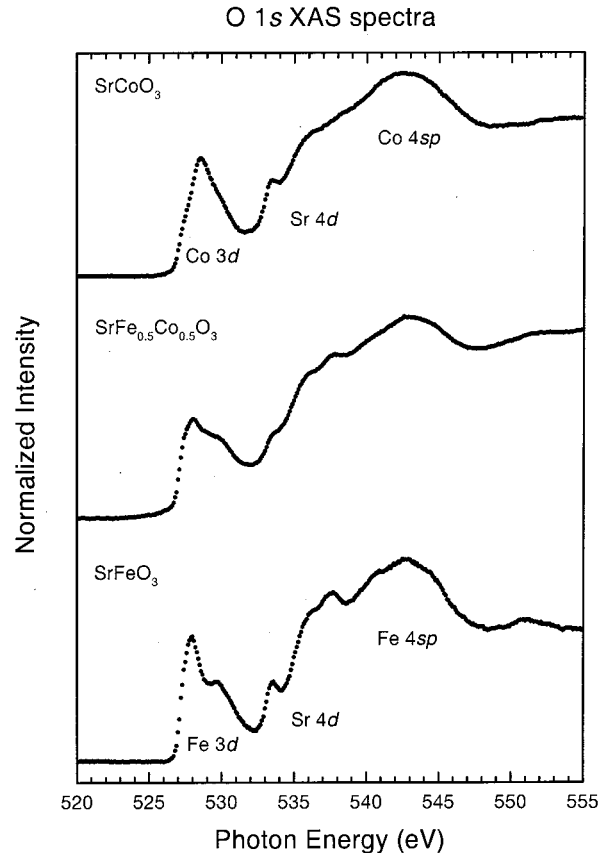


FIG. 3. O $1s$ x-ray absorption spectra of SrFeO_3 , $\text{SrFe}_{0.5}\text{Co}_{0.5}\text{O}_3$, and SrCoO_3 (dots).

approximately 5.9, is much larger than the purely ionic value 5.0. This indicates that the covalent contribution to the bonding in SrCoO_3 is even larger than in SrFeO_3 .

The Co $2p$ XAS spectrum of $\text{SrFe}_{0.5}\text{Co}_{0.5}\text{O}_3$ presents only minor changes with respect to SrCoO_3 . The absence of changes indicates that the Co ions are not drastically affected in $\text{SrFe}_{0.5}\text{Co}_{0.5}\text{O}_3$. This means that the formally tetravalent Co^{4+} ions remains mostly in the intermediate-spin state. The mixed material is in the negative-charge-transfer regime with a considerable amount of O $2p$ holes, and finally the covalent contribution to the bonding in $\text{SrFe}_{0.5}\text{Co}_{0.5}\text{O}_3$ is considerably large. Further support for these conclusions is provided by the analysis of the O $1s$ XAS spectra below.

C. O $1s$ XAS spectra

Figure 3 shows the O $1s$ x-ray absorption spectra of SrFeO_3 , $\text{SrFe}_{0.5}\text{Co}_{0.5}\text{O}_3$, and SrCoO_3 . The spectra correspond to transitions from the O $1s$ to unoccupied O $2p$ states in the conduction band. These empty O $2p$ states reflect, through the oxygen-metal hybridization, bands of mostly metal character.⁹ The first peaks at threshold corresponds to the Fe-Co $3d$ band region, the rising structure around 535 eV corresponds to the Sr $4d$ band region, and the bumps around 540–545 eV correspond to the Fe-Co $4sp$

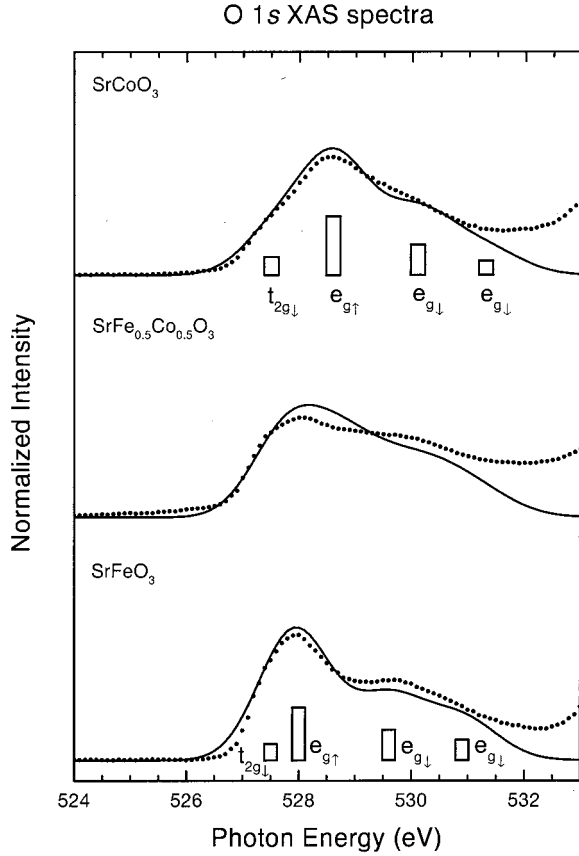


FIG. 4. Metal $3d$ region of the O $1s$ XAS spectra of SrFeO_3 , $\text{SrFe}_{0.5}\text{Co}_{0.5}\text{O}_3$, and SrCoO_3 (dots) compared to cluster model calculations (solid lines).

band region. These assignments are consistent with previous analysis of the SrMnO_3 and SrFeO_3 spectra.¹⁰

Figure 4 shows in more detail the metal $3d$ band region of SrFeO_3 , $\text{SrFe}_{0.5}\text{Co}_{0.5}\text{O}_3$, and SrCoO_3 . These regions can be analyzed using cluster model calculations including charge-transfer configurations. The method of calculation follows that used in the closely related SrMnO_3 and CaMnO_3 compounds.^{14,15} The metal $3d$ band region spectra corresponds to $3d^{n+1}\underline{L} \rightarrow \underline{c}3d^{n+1}$ transitions, where \underline{c} denotes an O $1s$ core hole. The energies of the final state configurations are related to the value of the Δ , U , and T_σ parameters. The model parameters used here were the same used in the previous analysis of the metal $2p$ XAS spectra.

The relative energy of the transitions is mostly given by the energies of the various $3d^{n+1}$ final state configurations. The relative intensities of the transitions is mainly given by the occupations of the $3d^{n+1}\underline{L}$ terms in the ground state. The Racah parameters (B and C) were reduced to 60–70% of their initial Hartree-Fock value (this reduction takes into account the extra screening of the O $2p$ ligand holes in the ground state). The crystal field splitting was estimated from LSDA calculations of pure SrFeO_3 and SrCoO_3 .¹⁶ The absolute energy and intensity of the calculations were adjusted so as to match the experimental peaks.

Figure 4 shows the calculations for the metal $3d$ band region of the SrFeO_3 and SrCoO_3 compounds. The calculation for the SrFeO_3 compound corresponds to $3d^4\underline{L} \rightarrow \underline{c}3d^4$ transitions in O_h symmetry. The relative energy and intensity of the calculated spectrum is in reasonably agreement with the experiment. In addition, the calculated spectral weight for SrFeO_3 is also in agreement with previous LSDA calculations.¹⁶ The calculated DOS exhibited a sharp minority t_{2g} band at the Fermi level, a broad majority e_g band across E_F , and a broad minority e_g band above E_F .

The calculation for the SrCoO_3 compound corresponds to $3d^5\underline{L} \rightarrow \underline{c}3d^5$ transitions in O_h symmetry. The calculated spectrum is in reasonably agreement with the experiment and previous LSDA calculations.¹⁶ This provides further support for the intermediate-spin interpretation of the Co $2p$ XAS spectrum above. The calculated DOS exhibited a sharp minority t_{2g} band at the Fermi level, a broad majority e_g across E_F , and a broad minority e_g band above E_F . The main difference with respect to SrFeO_3 is that the majority e_g band in SrCoO_3 is further apart from E_F (in fact, SrCoO_3 is close to be a half-metallic ferromagnet with a minimum in the majority e_g band at E_F).

The calculation for the $\text{SrFe}_{0.5}\text{Co}_{0.5}\text{O}_3$ compound is a linear combination of SrFeO_3 and SrCoO_3 . The relative energy and intensity of the calculated spectrum is in fair agreement with the experiment. We note that the intensity of the $e_{g\uparrow}$ peak is overestimated and that of the $e_{g\downarrow}$ peaks is underestimated. At first sight, these could be attributed to a partial transformation of some Co ions into a high-spin $t_{2g}^3e_g^2$ (6A_1) state. However, this is unlikely because the Co $2p$ XAS spectrum shows that most of the Co ions remains in the intermediate-spin $t_{2g}^4e_g^1$ (4T_1) state. On other hand, changes in the Fe ions can be ruled out because the high-spin $t_{2g}^3e_g^1$ (5E) state is rather stable. The differences are attributed to changes in the ground state of O ions located between Fe and Co ions.

D. Physical properties

1. Tendency to ferromagnetism in SrFeO_3

The SrFeO_3 compound is antiferromagnetic with a screw structure along the propagation wave vector $\mathbf{k} \parallel \langle 111 \rangle$. The Heisenberg-like exchange interactions estimated from the analysis of paramagnetic neutron scattering are $J_1 = 1.2$ meV, $J_2 = -0.2$ meV, and $J_4 = -0.3$ meV.⁵ The screw structure is due to the competition between the ferromagnetic nearest-neighbor interaction J_1 , and the antiferromagnetic second- and fourth-nearest-neighbor interactions J_2 and J_4 , respectively. We note that the magnitude of the propagation wave vector in SrFeO_3 ($|\mathbf{k}| \cong 0.135a^*$) is relatively small.⁵ In turn, this implies that the corresponding wavelength of the magnetic screw structure is relatively large. In fact, the relative phase angle between two adjacent spins along the $\langle 111 \rangle$ direction (40°) is rather small. This fact can be understood taking into account that the FM interaction is much larger than the AFM interactions. All this suggests that the magnetic structure of SrFeO_3 is on the verge of becoming ferromagnetic, see below.

2. (Half-metallic) ferromagnetism in SrCoO₃?

The microscopic origin of the ferromagnetism in the SrCoO₃ compound is not completely clear at the moment. The results shows that the electronic structure of this material derives from the intermediate-spin $t_{2g}^4 e_g^1$ (4T_1) state. The ground state is not only given by the $3d^5$ configuration, but it contains also a considerable $3d^6\bar{L}$ weight. Potze *et al.* proposed that the ferromagnetism in SrCoO₃ was due to a double-exchange-like mechanism,¹³ which involves Co-O-Co interactions between partially filled e_g states mediated by the corresponding O $2p$ holes. Band structure calculations of SrCoO₃, however, shows a minimum in the majority e_g band at the Fermi level¹⁶ (this is also supported by the above cluster model calculations which show a majority e_g peak far away from E_F). So, in fact, SrCoO₃ might be a half-metallic ferromagnet such as the double-perovskite system Sr₂FeMoO₆.

3. Absence of Jahn-Teller distortion in SrFeO₃

The ground state of the Fe⁴⁺ ions in the cubic perovskite SrFeO₃ derives from the high-spin $t_{2g}^3 e_g^1$ (5E) state. At first sight, it is surprising that this double-degenerate state does not exhibit a (cooperative) Jahn-Teller distortion. This apparent discrepancy can be reconciled taking into account the relatively large occupancy of the $3d^5\bar{L}$ configuration. In fact, the ground state of SrFeO₃ is dominated by the $3d^5\bar{L}$ configuration (58%) and not by the $3d^4$ configuration (36%). The main $3d^5$ component of the $3d^5\bar{L}$ configuration is given by the high-spin $t_{2g}^3 e_g^2$ (6A_1) state which inhibits the distortion. The isoelectronic Mn³⁺ ions in LaMnO₃ are also in a high-spin $t_{2g}^3 e_g^1$ (5E) state and present a Jahn-Teller distortion, but in this case, the ground state (given by 55% $3d^4$, 40% $3d^5\bar{L}$, and 5% $3d^6\bar{L}^2$) is more ionic than in SrFeO₃. This indicates that a strong covalency could eventually quench Jahn-Teller distortions (and/or charge-ordering phenomena).

4. Magnetic moment at the oxygen sites

The ground state of the SrFeO₃ and SrCoO₃ compounds contains a considerable amount of O $2p$ hole character. This follows from the relatively large occupancy of the charge-transfer configurations $3d^{n+1}\bar{L}$ in the ground state. In turn, this fact helps to explain the relatively large magnetic moment observed at the O sites in both compounds. The magnetic moment at the O sites derived from neutron measurements is approximately $0.1\mu_B$ in both cases.¹⁷ A magnetic moment at the O sites was also observed in O $1s$ magnetic-circular-dichroism results in SrCoO₃.¹⁸ The magnetic moment obtained from LSDA calculations is about $0.14\mu_B$ for SrFeO₃ and $0.19\mu_B$ for SrCoO₃.¹⁶ The larger moment for SrCoO₃ can be understood taking into account that SrCoO₃ is more covalent than SrFeO₃ (the occupancy of the charge transfer $3d^{n+1}\bar{L}$ configuration in SrCoO₃, 67%, is larger than that in SrFeO₃, 58%).

5. Origin of the ferromagnetism in SrFe_{1-x}Co_xO₃

The microscopic origin of the ferromagnetism in the SrFe_{1-x}Co_xO₃ compound is not completely understood yet.

As indicated above, the dominating interactions in the starting member of the series, SrFeO₃, are ferromagnetic.³ In fact, a relatively small amount of Co, $x \geq 0.2$, is enough to turn the SrFe_{1-x}Co_xO₃ material ferromagnetic.⁵ The main question left is how the Co presence quench the residual antiferromagnetic interactions in SrFeO₃.³ The most invoked possibilities would be the double-exchange mechanism and half-metallic ferromagnetism. The first is related to a model of fluctuations between (localized) spins, whereas the second derives from (itinerant) band structure calculations.

We argue that a mechanism based on double-exchange is unlikely in the mixed SrFe_{1-x}Co_xO₃ compound, simply because the potential felt by the supposedly active e_g electrons at the Fe and Co sites is different (although, we must note here that a double-exchange mechanism remains a valid possibility in pure SrCoO₃).¹³ The second possibility is that the Co ions induce a minimum at E_F in the majority e_g band of SrFe_{1-x}Co_xO₃, eventually turning the material ferromagnetic as in the alternative half-metallic ferromagnetism scenario. In this sense, the ferromagnetism in SrFe_{1-x}Co_xO₃ resembles the half-metallic ferromagnetism in Sr₂FeMoO₆,² and not the double-exchange ferromagnetism often proposed for manganites, such as La_{1-x}Ca_xMnO₃.¹

6. Magnetoresistance mechanism in SrFe_{1-x}Co_xO₃

The origin of the magnetoresistance mechanism in the SrFe_{1-x}Co_xO₃ compound⁶ remains unclear at the moment. The main possibilities would be based on the double-exchange mechanism and on tunneling between ferromagnetic phases. Again, the double-exchange mechanism is not possible due to the potential differences between the Fe and Co sites. Tunneling between ferromagnetic phases, within a phase separation scenario,¹⁹ seems to be a more likely explanation. In fact, this scenario is supported by previous studies of the magnetic properties of the Fe-rich phase of SrFe_{1-x}Co_xO₃. These studies suggest that SrFe_{1-x}Co_xO₃ ($x \leq 0.15$) is composed by ferromagnetic islands coupled antiferromagnetically.⁵

We note that large magnetoresistance in Sr₂FeMoO₆ is observed in polycrystalline samples and not in single crystals.² This was interpreted as being due to tunneling between half-metallic ferromagnetic grains in the polycrystalline samples.² In this sense, the origin of the magnetoresistance in SrFe_{1-x}Co_xO₃ seems to be similar to the origin in Sr₂FeMoO₆,² and has less in common with double-exchange based explanations usually proposed for manganites such as La_{1-x}Ca_xMnO₃.¹ It remains to be checked if the inhomogeneities in SrFe_{1-x}Co_xO₃ are intrinsic or due to the microstructure of the samples, this could be eventually tested by means of magnetotransport measurements in single crystals of SrFe_{1-x}Co_xO₃.

7. Negative charge-transfer character of SrFe_{1-x}Co_xO₃

The analysis of the spectra above shows that the SrFe_{1-x}Co_xO₃ compound is in the negative charge-transfer

regime.¹² This means that the ionic state is not really Fe^{4+} and Co^{4+} , but rather that the charge state is compensated by O $2p$ holes (in terms of the CI cluster model, the occupation of the $3d^{n+1}\underline{L}$ configuration is larger than that of the $3d^n$ configuration). Therefore, $\text{SrFe}_{1-x}\text{Co}_x\text{O}_3$ illustrates both ferromagnetism and magneto-resistance in a negative charge-transfer material, and confirms that the ground state of $\text{SrFe}_{1-x}\text{Co}_x\text{O}_3$ is qualitatively different from manganites¹ and double perovskites.² We note that $\text{La}_{1-x}\text{Ca}_x\text{MnO}_3$ is in a mixed charge-transfer/Mott-Hubbard regime and has a dominating $3d^n$ configuration.¹⁴ The situation is less clear in $\text{Sr}_2\text{FeMoO}_6$, although recent XAS studies show that the Fe ions are indeed in a Fe^{3+} state, with a mixed pd -metal ground state which is mostly dominated by the first ionic $3d^n$ configuration.²⁰

IV. SUMMARY AND CONCLUSIONS

In summary, we studied the relation between the electronic structure and the physical properties of $\text{SrFe}_{1-x}\text{Co}_x\text{O}_3$. The main technique used in the study was Fe $2p$, Co $2p$, and O $1s$ x-ray absorption spectroscopy (XAS). The experimental spectra were analyzed in terms of the configuration-interaction cluster model calculation. The analysis of the spectra shows that both SrFeO_3 and SrCoO_3 are in the negative-charge transfer regime (this means that their ground states are mostly covalent and contain consid-

erable O $2p$ hole character). SrFeO_3 is in a high-spin state and SrCoO_3 in an intermediate-spin state stabilized by strong hybridization. The local electronic structure and the corresponding spin state are mostly preserved in $\text{SrFe}_{1-x}\text{Co}_x\text{O}_3$. The relatively large O $2p$ hole weight in the ground state explains the absence of Jahn-Teller distortions, as well as the relatively large value of the magnetic moment observed at the O sites in these materials. The origin of the magnetoresistance in the $\text{SrFe}_{1-x}\text{Co}_x\text{O}_3$ compound remains unclear at the moment. The double-exchange mechanism seems unlikely due to the difference in the Fe and Co on-site energies. Tunneling between ferromagnetic phases, within a phase separation scenario, is a more likely explanation. $\text{SrFe}_{1-x}\text{Co}_x\text{O}_3$ illustrates both ferromagnetism and magnetoresistance in a negative charge-transfer material. The ground state is qualitatively different from manganites, such as $\text{La}_{1-x}\text{Ca}_x\text{MnO}_3$, and double-perovskites, such as $\text{Sr}_2\text{FeMoO}_6$.

ACKNOWLEDGMENTS

We would like to thank the technical staff of the LNLS for their helpful assistance during the measurements. We would like to thank D.D. Sarma for useful comments on the manuscript. This work was partially supported by CNPq, PRONEX, LNLS, Fundación Antorchas and Fundação Araucaria.

-
- ¹R. von Helmut, J. Wecker, B. Holzapfel, L. Schultz, and K. Samwer, *Phys. Rev. Lett.* **71**, 2331 (1993); Y. Tokura, A. Urushibara, Y. Morimoto, T. Arima, A. Asamitsu, G. Kido, and N. Furukawa, *J. Phys. Soc. Jpn.* **63**, 3931 (1994); S. Jin, T.H. Tiefel, M. McCormack, R.A. Fastnacht, P. Ramesh, and L.H. Chen, *Science* **264**, 413 (1994); P. Schiffer, A.P. Ramirez, W. Bao, and S.W. Cheong, *Phys. Rev. Lett.* **75**, 3336 (1995).
- ²K.I. Kobayashi, T. Kimura, H. Sawada, K. Terakura, and Y. Tokura, *Nature (London)* **395**, 677 (1998); B. Garcia-Landa, C. Ritter, M.R. Ibarra, J. Blasco, P.A. Algarabel, R. Mahendiran, and J. Garcia, *Solid State Commun.* **110**, 435 (1999); H.Q. Yin, J.S. Zhou, J.P. Zhou, R. Dass, J.T. McDevitt, and J.B. Goodenough, *Appl. Phys. Lett.* **75**, 2812 (1999); Y. Tomioka, T. Okuda, Y. Okimoto, R. Kumai, K.I. Kobayashi, and Y. Tokura, *Phys. Rev. B* **61**, 422 (2000).
- ³J.B. MacChesney, R.C. Sherwood, and J.F. Potter, *J. Chem. Phys.* **43**, 1907 (1965); T. Takeda, Y. Yamaguchi, and H. Watanabe, *J. Phys. Soc. Jpn.* **33**, 967 (1972); A. Wattiaux, L. Fournes, A. Demourgues, N. Bernabén, J.C. Grenier, and M. Pouchard, *Solid State Commun.* **77**, 489 (1991).
- ⁴H. Watanabe, *J. Phys. Soc. Jpn.* **12**, 515 (1957); H. Taguchi, M. Shimada, and M. Koizumi, *Mater. Res. Bull.* **17**, 1225 (1978); P. Bezdzicka, A. Wattiaux, J.C. Grenier, M. Pouchard, and P. Hagenmuller, *Z. Anorg. Allg. Chem.* **619**, 7 (1993).
- ⁵T. Takeda and H. Watanabe, *J. Phys. Soc. Jpn.* **33**, 973 (1972); P. Bezdzicka, L. Fournes, A. Wattiaux, J.C. Grenier, and M. Pouchard, *Solid State Commun.* **91**, 501 (1994); S. Kawasaki, M. Takano, and Y. Takeda, *J. Solid State Chem.* **121**, 174 (1996).
- ⁶P.D. Battle, M.A. Green, J. Lago, A. Mihut, M.J. Rosseinsky, L.E. Spring, J. Singleton, and J.F. Vente, *Chem. Commun. (London)* **9**, 987 (1998); I.M. Marshall, S.J. Blundell, A. Husmann, Th. Jestädt, B.W. Lovett, F. L Pratt, J. Lago, P.D. Battle, and M.J. Rosseinsky, *Physica B* **289-290**, 89 (2000); A. Maignan, C. Martin, N. Nguyen, and B. Raveau, *Solid State Sci.* **3**, 57 (2001); Y.M. Zhao, R. Mahendiran, N. Nguyen, B. Raveau, and R.H. Yao, *Phys. Rev. B* **64**, 024414 (2001).
- ⁷S. Kawasaki, M. Takano, and Y. Takeda, *J. Solid State Chem.* **121**, 174 (1996).
- ⁸M. Abbate, J.B. Goedkoop, F.M.F. de Groot, M. Grioni, J.C. Fuggle, S. Hofmann, H. Petersen, and M. Sacchi, *Surf. Interface Anal.* **18**, 65 (1992).
- ⁹M. Abbate, H. Pen, M.T. Czyzyk, F.M.F. de Groot, J.C. Fuggle, Y.J. Ma, C.T. Chen, F. Sette, A. Fujimori, Y. Ueda, and K. Kosuge, *J. Electron Spectrosc. Relat. Phenom.* **62**, 185 (1993).
- ¹⁰M. Abbate, F.M.F. de Groot, J.C. Fuggle, A. Fujimori, O. Strebler, F. Lopez, M. Domke, G. Kaindl, G.A. Sawatzky, M. Takano, Y. Takeda, H. Eisaki, and S. Uchida, *Phys. Rev. B* **46**, 4511 (1992).
- ¹¹A.E. Bocquet, A. Fujimori, T. Mizokawa, T. Saitoh, H. Namatame, S. Suga, N. Kimizuka, Y. Takeda, and M. Takano, *Phys. Rev. B* **45**, 1561 (1992).
- ¹²T. Mizokawa, H. Namatame, A. Fujimori, K. Akeyama, H. Kondoh, H. Kuroda, and N. Kosigi, *Phys. Rev. Lett.* **67**, 1638 (1991).
- ¹³R.H. Potze, G.A. Sawatzky, and M. Abbate, *Phys. Rev. B* **51**, 11 501 (1995).
- ¹⁴T. Saitoh, A.E. Bocquet, T. Mizokawa, H. Namatame, A. Fujimori,

- M. Abbate, Y. Takeda, and M. Takano, *Phys. Rev. B* **51**, 13 942 (1995).
- ¹⁵G. Zampieri, F. Prado, A. Caneiro, J. Briatico, M.T. Causa, M. Tovar, B. Alascio, M. Abbate, and E. Morikawa, *Phys. Rev. B* **58**, 3755 (1998).
- ¹⁶S.M. Jaya, R. Jagadish, R.S. Rao, and R. Asokamani, *Phys. Rev. B* **43**, 13 274 (1991); S. Mattar, G. Demazeau, P. Mohn, V. Eyert, and S. Najm, *Eur. J. Solid State Inorg. Chem.* **31**, 615 (1994); S.F. Mattar, A. Villesuzanne, and M. Uhl, *J. Mater. Chem.* **6**, 1785 (1996).
- ¹⁷T. Takeda, T. Watanabe, S. Komura, and H. Fujii, *J. Phys. Soc. Jpn.* **56**, 731 (1987).
- ¹⁸J. Okamoto, H. Miyauchi, T. Sekine, T. Shidara, T. Koide, K. Amemiya, A. Fujimori, T. Saitoh, A. Tanaka, Y. Takeda, and M. Takano, *Phys. Rev. B* **62**, 4455 (2000).
- ¹⁹S. Yunoki, J. Hu, A.L. Malvezzi, A. Moreo, N. Furukawa, and E. Dagotto, *Phys. Rev. Lett.* **80**, 845 (1998); A. Moreo, S. Yunoki, and E. Dagotto, *Science* **283**, 2034 (1999); M. Uehara, S. Mori, C.H. Chen, and S.W. Cheong, *Nature (London)* **399**, 560 (1999); M. Fath, S. Freisem, A.A. Menovsky, Y. Tomioka, J. Aarts, and J.A. Mydosh, *Science* **285**, 1540 (1999).
- ²⁰S. Ray, A. Kumar, D.D. Sarma, R. Cimino, S. Turchini, S. Zennaro, and N. Zema, *Phys. Rev. Lett.* **87**, 097204 (2001); M.S. Moreno, J.E. Gayone, M. Abbate, A. Caneiro, D. Niebieskikwiat, R.D. Sanchez, A. de Siervo, R. Landers, and G. Zampieri, *Solid State Commun.* **120**, 161 (2001).